

HIGH ACCELERATION ABILITY OF A HOMEMADE 8-CH MOUSE PHASED ARRAY SUGGESTS THE POSSIBILITY FOR EPI-BASED FUNCTIONAL STUDIES OF MICE MODELS USING A STANDARD 3T HUMAN SCANNER

Hui Han¹, John Stager¹, Wei Cao², Miguel Navarro³, Fraser Robb³, Junghun Cho¹, Nozomi Nishimura⁴, Chris Schaffer⁴, Valerie Reyna¹, Yi Wang¹, and Wen-Ming Luh¹

¹Cornell MRI Facility, Cornell University, Ithaca, New York, United States, ²Tongji Hospital, Huazhong University of Science and Technology, Hubei, China, ³GE Healthcare, Ohio, United States, ⁴Biomedical Engineering, Cornell University, Ithaca, New York, United States

TARGET AUDIENCE: Who interested in preclinical studies (anatomical and functional imaging) using clinical scanners, RF coils, parallel imaging, B₀ shimming.

PURPOSE: There is an increasing need for preclinical anatomical and functional studies in recent years^{1,2}. Albeit the rather limited gradient and main field strengths, clinical scanners are advantageous in readily equipped multi-channel receivers, versatile sequence options, and more importantly their widespread availability for many facilities without extra budget for both acquisition and maintenance of expensive small animal imaging systems. Here we show a homemade 8-ch mouse phased array interfaced to a standard 3T human scanner. A fact one may easily neglect is that the small imaging space allows for an excellent parallel imaging ability even for a low coil-element count (8) being used, which is a different scenario for a human coil with a larger imaging space. We are to apply this coil in detecting hemorrhage in mouse brain using quantitative susceptibility mapping (QSM)³. As an initial trial, using single-shot gradient echo EPI with parameters tailored to fMRI, also shows the possibility for functional studies of mice models by taking advantage of multi-channel receivers, which provides a weight to compensate for the limited gradient strength of clinical systems. To our best knowledge, this is one of few first demonstrations to attempt fMRI of mice on a clinical system.

METHODS: 8 circular elements were arranged in 2 rings with each ring having 4 loops (4 cm diameter) on a 38 mm diameter fiberglass tube (Fig. 1). Each loop had two gaps with one gap for placing a capacitive tuning circuit and the other connected to a printed circuit board, which contained a matching and preamplifier network. Also an active detuning circuit was forward biased during RF transmission. Each loop was overlapped and geometrically decoupled to its 4 nearest neighbors and next-nearest neighboring loops were decoupled using low impedance pre-amplifier decoupling. A standard coil plug was used to connect the coil to the scanner. A similar size birdcage coil was also built for SNR comparison. Bench testing was performed including tuning, matching, geometrical and pre-amp decoupling, and active decoupling of each channel using a network analyzer and a custom made test rig.

All experiments were performed on a state-of-the-art 3 T whole-body MRI scanner (GE MR750), equipped with 32 RF receivers. The gradient system has 50 mT/m maximum amplitude gradients and a maximum gradient slew rate of 200 mT/m/ms. Body coil was used for RF excitation. A 35-ml phantom was made for SNR and G-factor measurements using a methodology⁴, for which FOV was set smallest possible. An adult mouse was sacrificed due to the mouse setup and review protocol required for live mice currently in progress. Anatomical images were acquired using an acceleration factor $R = 2$ for fast spin echo (FSE) proton density weighted images and $R = 3 \times 2$ for 3D FSE CUBE T₂ images (both 32 slices, matrix size 192×192), with corresponding acquisition times 1.92 min and 2.83 min. GRAPPA and SENSE were used for reconstructing anatomical and EPI images, respectively. The TEs for single-shot gradient EPI were 91ms, 49ms, 34ms, and 27ms for R from 1 to 4, respectively. EPI matrix size was 120×120 and voxel size 0.5×0.5×0.8 mm.

RESULTS: Bench tests showed geometrical decoupling of nearest neighbor loops from -18 dB to -25 dB with an average of -21 dB, which was further improved by pre-amp decoupling of 21 dB. The overall mutual coupling for the entire system ranged from -20 dB to -38 dB (mean -26 dB). An active decoupling of above 40 dB was achieved for each channel. The SNR was comparable to the size matched birdcage with 0.9-fold at the center of the phantom and 2-fold at the surface of the phantom. Fig. 2 shows the inverse G-factor maps. The mean / maximum G-factors are 1.12/1.37, 1.32/1.81, 2.54/5.26 for $R = 2 \times 2$, 3×2 , 3×3 , respectively. Fig. 4B&C show the potential of the array for highly accelerated imaging. Fig. 3D show the EPI images with R from 1 to 4.

DISCUSSION and CONCLUSION: The highly accelerated imaging ability for a low channel count (8) mouse array inherently lies in that tissues in a small imaging space can be well discriminated by sensitivity encoding⁵ contributed from all the coils. In contrast, for a human coil (e.g., 32-ch head coil), the region of interest is well seen only by the nearby a few coils albeit a high total channel count. As a result, an 8-ch mouse coil provides the acceleration ability comparable to a 32-ch human coil. For the same reason, a mouse coil with a higher channel count, such as a 20-ch array arranged in 4 rows and 5 loops per row², may not provide greatly improved acceleration ability compared to an 8-ch coil although it does provide an extend FOV coverage advantageous for whole mouse imaging. The construction was however much more complicated and the cost more than doubled. Most of users expressed interests on small ROIs such as the mouse brain or spinal cord.

We have not found any EPI or functional studies reported for mice models using clinical scanners. This is understood because at least 4 times lower gradient strength elongates the readout times by 4 times compared to animal scanners, in addition to a halved SNR, which led to severe signal dropout and image distortion in Fig. 3D using $R=1-2$. Apparently the prolonged TEs for $R=1-2$ were due to the limited gradient bandwidths. However, multiple receivers in clinical scanner may largely compensate for such disadvantages and high acceleration $R=3-4$ greatly alleviated this problem as shown in Fig. 3D. Image quality can be further improved by multi-coil local shimming using the integrated Shim/RF array⁶ currently under development. The potentials demonstrated deserve further studies considering the trivial cost for a multi-ch coil versus a dedicated small animal system in addition to its high maintenance expense. The potentials of this coil will be further verified by more users.

REFERENCES: 1. Aradi M et al. J Neuroradiology 2011;38:90-97. 2. Boris K et al. Magn Reson Med. 2011;66:584-595. 3. Wang Y and Liu T. Magn Reson Med. 2014;DOI:10.1002/mrm.25358. 4. Reeder SB et al. Magn Reson Med. 2005;54:748-754. 5. Pruessmann KP et al. Magn Reson Med. 1999;42:952-962. 6. Han H et al. Magn Reson Med. 2013;70:241-247.

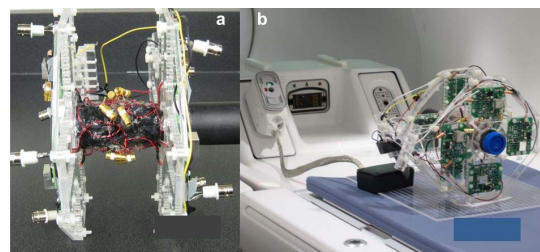


Fig. 1: 8-ch mouse coil in test (a) and interfaced to 3T MR750 (b).

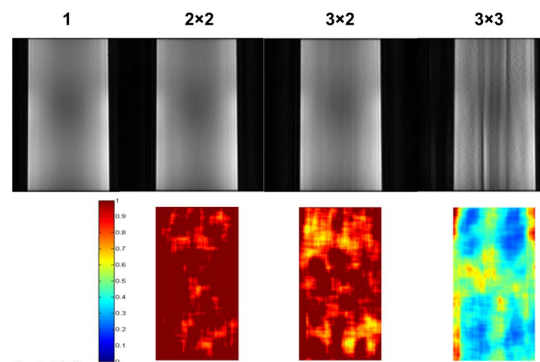


Fig. 2: Inverse G-factor maps of Sagittal phantom images using two-dimensional acceleration direction (phase=A/P, slice=R/L).

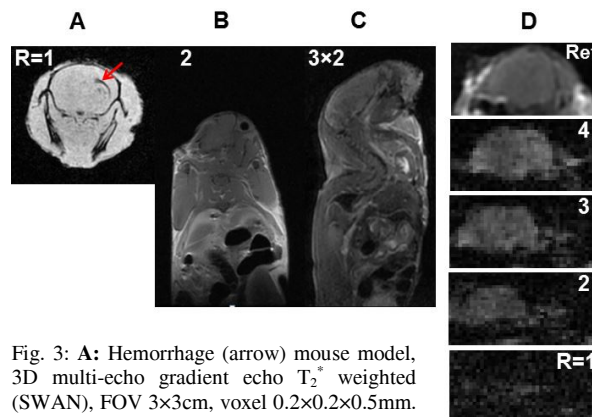


Fig. 3: **A:** Hemorrhage (arrow) mouse model, 3D multi-echo gradient echo T₂* weighted (SWAN), FOV 3×3cm, voxel 0.2×0.2×0.5mm. **B:** Proton density weighted, acceleration factor $R=2$ in A/P, 0.31×0.31×1mm. **C:** 3D fast spin echo T₂ weighted (CUBE), 0.31×0.31×1mm, $R= 3(A/P) \times 2(R/L)$. **D:** Single-shot gradient echo EPI images using parameters tailored to fMRI. A reference spin echo mouse brain image (top) followed by EPI (0.5×0.5×0.8mm) using acceleration factor of 1 to 4.